SPANDIDOS PUBLICATIONS

ONCOLOGY REPORTS 45: 448-458, 2021

Heat shock protein 90 as a molecular target for therapy in oral squamous cell carcinoma: Inhibitory effects of 17-DMAG and ganetespib on tumor cells

NAOKI SHIRAISHI, TAKESHI ONDA, KAMICHIKA HAYASHI, KAORU ONIDANI, KATSUHITO WATANABE, SHOICHI SEKIKAWA and TAKAHIKO SHIBAHARA

Department of Oral and Maxillofacial Surgery, Tokyo Dental College, Mihama-ku, Chiba 261-8502, Japan

Received October 24, 2019; Accepted October 2, 2020

DOI: 10.3892/or.2020.7873

Abstract. Heat shock protein 90 (HSP90) expression is upregulated in numerous types of cancer. However, its role as a candidate for molecular targeted therapy in oral squamous cell carcinoma (OSCC) cells is poorly understood. In the present study, a common upstream search was performed using molecular network analysis software for proteins with expression abnormalities that were found in a proteomic analysis of six OSCC cell lines. HSP90 was identified as a target protein. In clinical samples, high frequencies of HSP90-high expression were detected via immunohistochemistry (26/58; 45%). Furthermore, the HSP90 expression status was associated with cervical lymph node metastasis (P=0.015). Furthermore, the potential of HSP90 as a candidate for molecular targeted therapy in OSCC cells was investigated using the HSP90 inhibitors 17-dimethylaminoethylamino-17-demethoxygeldanamycin (17-DMAG) and ganetespib. KON cells, which strongly express HSP90, were treated with the HSP90 inhibitors. The numbers of living cells in the 17-DMAG and ganetespib-treated groups were lower than those in the non-treated group. The cells treated with the inhibitors demonstrated reduced cell viability and migration, and this was associated with markedly decreased levels of the HSP90 target proteins EGFR, phospho-EGFR, phospho-MEK and phospho-MAPK in the treated groups compared with the non-treated group. To the best of our knowledge, this was the first study to investigate the effects of 17-DMAG and ganetespib on OSCC cells. The present results indicated the potential of HSP90 as a useful candidate for molecular targeted therapy in OSCC. However, additional studies with larger sample sizes are required to confirm these findings.

Correspondence to: Dr Takeshi Onda, Department of Oral and Maxillofacial Surgery, Tokyo Dental College, 1-2-2 Masago, Mihama-ku, Chiba 261-8502, Japan
E-mail: ondatake@tdc.ac.jp

Key words: heat shock protein 90, oral squamous cell carcinoma, two-dimensional fluorescence difference gel electrophoresis, 17-dimethylaminoethylamino-17-demethoxygeldanamycin, ganetespib

Introduction

Oral cancer affects various parts of the oral cavity, such as the tongue, gingiva, floor of the mouth and buccal mucosa, and is the sixth most common malignant neoplasm worldwide (1). Oral squamous cell carcinoma (OSCC) is the most frequently occurring malignancy in the oral cavity (1). Although significant advances in the development of comprehensive and multimodality therapies for OSCC have been achieved over the past few decades, the long-term survival rates have remained relatively unchanged, particularly in patients with advanced lesions (2). Locoregional relapse and cervical lymph node metastasis are the most prevalent and significant factors that affect the prognosis of patients with OSCC (2). Although the initiation and progression of OSCC are closely associated with the activation of aberrant oncogenes, inactivation of tumor suppressors and other epigenetic abnormalities, the molecular carcinogenesis of OSCC has not yet been elucidated in detail, and this has hindered the development of potent and sensitive biomarkers, and therapeutic strategies (3). Therefore, the underlying molecular mechanisms and novel therapeutic targets need to be identified in order to improve the prognosis of patients with OSCC. Tumor biomarkers that accurately reflect tumor cell characteristics or could be used as treatment targets have been the focus of continuing research. Two-dimensional fluorescence difference gel electrophoresis (2D-DIGE) has been employed for protein separation (4), and proteomic approaches have contributed to the identification of biomarkers in various types of cancer (5,6). However, they have not yet been extensively applied to oral cancer (7,8). In the present study, the protein expression profiles in normal epidermal keratinocytes and OSCC cell lines were examined using 2D-DIGE and liquid chromatography tandem-mass spectrometry (LC-MS/MS). A common upstream search was performed for proteins with expression abnormalities in a proteomic analysis of OSCC cells. The results obtained identified heat shock protein 90 (HSP90) as a target that regulated the functional maintenance and stability of numerous client proteins, which serve important roles in OSCC cell proliferation and survival.

The molecular chaperone HSP90 is involved in regulating the maturation and functional stability of an extensive array

of cellular client proteins, an activity that is often exploited by cancer cells to confer an aberrant proliferative, survival and/or metastatic potential (9,10). The HSP90 machinery functions as a biochemical buffer for a number of oncogenic signaling proteins that have been causally implicated in various human tumors; mutant oncoproteins have been previously demonstrated to rely on the chaperone (11,12). The functional inhibition of HSP90 results in the simultaneous degradation of hundreds of client proteins, thereby providing a mechanism to concomitantly disrupt multiple oncogenic signaling cascades through a single molecular target (13). The pharmacological blockade of HSP90 has emerged as an innovative approach for the development of novel antineoplastic agents (13). Therefore, the potential of HSP90 as a candidate for molecular targeted therapy was investigated in OSCC cells treated with HSP90 inhibitors in the present study. In addition, a functional analysis of the HSP90 protein was conducted using *in vitro* assays, and the relationships between the expression levels of this protein and clinicopathological factors, as well as the prognosis of patients, were assessed using immunohistochemistry (IHC).

Materials and methods

Cells. The OSCC KON, OSC-20, HSC-3, HSC-4, SAS and Ca9-22 cell lines were obtained from the Japanese Collection of Research Bioresources Cell Bank. The spontaneously transformed immortal keratinocyte cell line, HaCaT (cat. no. 300493), was obtained from CLS Cell Lines Service GmbH. All cell lines were maintained at 37˚C in a humidified atmosphere of 5% CO_2/95% air. FBS was purchased from Sigma-Aldrich; Merck KGaA. The KON cells were cultured in DMEM (Sigma-Aldrich; Merck KGaA) supplemented with 10% FBS and 50 U/ml penicillin and streptomycin (Sigma-Aldrich; Merck KGaA). The OSC-20 and SAS cells were cultured in DMEM/F-12 medium (Sigma-Aldrich; Merck KGaA) with 10% FBS and 50 U/ml penicillin and streptomycin. The HSC-3, HSC-4 and Ca9-22 cells were cultured in minimum essential medium (Sigma-Aldrich; Merck KGaA) supplemented with 10% FBS and 50 U/ml penicillin and streptomycin. The HaCaT cells, which were used as controls in the present study, were cultured in DMEM supplemented with 10% FBS and 50 U/ml penicillin and streptomycin. The culture medium was changed twice a week for all cells. It has been reported that the Ca9-22 cell line is contaminated with MSK-922 cells (14). Therefore, short tandem repeat (STR) analysis was performed and it was confirmed that the cell line used in the present study was not contaminated. STR analysis was performed by a third party (Promega Corporation) using the PowerPlex 16 kit (Promega Corporation) which analyses 16 independent genetic sites specific for human DNA that include the 13 CODIS loci, plus PENTA E, PENTA D and amelogenin (15).

2D-DIGE and image analysis. 2D-DIGE was performed as described previously (16,17). In brief, a common internal control sample was created by mixing a small portion from all protein samples used in the present study, and this was then labeled using a Cy3 fluorescent dye (CyDye DIGE Fluor saturation dye; GE Healthcare Bio-Sciences). Individual samples were labeled with Cy5 fluorescent dye (CyDye DIGE Fluor saturation dye; GE Healthcare Bio-Sciences). The protein samples were mixed together and separated using 2D-DIGE based on their isoelectric points and molecular weights. First-dimension separation was performed with an Immobiline DryStrip Gel (IPG; length, 24 cm; pH 3.0-10.0; GE Healthcare Bio-Sciences) and the Multiphor Electrophoresis System (GE Healthcare Bio-Sciences). The second-dimension separation was performed using a homemade gradient gel with GiantGelRunner (separation distance, 36 cm; Everseiko Corporation). The gels were scanned using a laser scanner (Typhoon Trio; GE Healthcare Bio-Sciences) at the appropriate wavelengths for Cy3 or Cy5 (Cy3: Excitation 532 nm, fluorescence 580 nm; Cy5: Excitation 633 nm, fluorescence 670 nm). The gel images were analyzed automatically using the DeCyder-BVA (biologic variation analysis) software (version 7.0; GE Healthcare Bio-Sciences). The statistical significance of each expression level was calculated using Student's t-test on the logged ratios.

Mass spectrometry analysis. Proteins (100 μg/lane) separated by 12% SDS-PAGE were visualized using SYPRO Ruby staining (Molecular Probes; Thermo Fisher Scientific, Inc.) at room temperature for 3 h. The peptide samples were excised from the gels and digested by trypsin using the In Gel Digest Kit (EMD Millipore) as described previously (18). Following the extraction of the peptides, the proteolytic peptide mixture was evaporated to ~5 ml, and 35 ml of 2% acetonitrile and 0.1% trifluoroacetic acid were added to the mixture, which was then subjected to an autosampler (HTC PAL; CTC Analytics AG) for nanoscale capillary LC-MS/MS analysis. A capillary LC system (Magic 2002; Bruker-Michrom, Inc.) coupled to an in-line nanoelectrospray mass spectrometer (LCQ Advantage; Thermo Fisher Scientific, Inc.) with a silica-coated glass capillary (PicoTip; New Objective, Inc.) was used. The analysis conditions were as follows: Ionization mode used, positive mode; column temperature, room temperature; flow rate, 2.5 μl/min. The samples were loaded in 5% acetonitrile with 0.1% formic acid. The gradient consisted of 6.4% acetonitrile for 5 min followed by 6.4 to 76.8% acetonitrile for 45 min. The spectra were collected as MS and MS/MS scans. The MS scan defined the ion composition at an m/z range of 450-2,000, and the MS/MS scan acquired the mass spectrum of the parental ion upon collision-induced dissociation. The collision-induced dissociation spectra acquired were then analyzed by direct inspection using the Mascot software program (version 2.2.04; Matrix Science, Inc.) as described previously (19,20).

Hierarchical clustering and molecular network analyses. Hierarchical clustering analysis of protein expression data was performed using the Multi Experiment View cluster software version 4.9.0 (21,22). A molecular network analysis was performed using the KeyMolnet® software version 5.8 (23), which encompasses the majority of relationships among human genes and proteins, molecules, diseases, pathways and drugs. This information is manually collected, carefully curated and regularly updated by expert biologists. The database is categorized into core contents, which are collected from selected review articles with the highest reliability and secondary contents, which are extracted from abstracts in the PubMed (https://pubmed.ncbi.nlm.nih.gov/) and Human Protein Reference databases (https://www.hprd.org/).

KeyMolnet® provides information on the corresponding molecules as a node on networks by importing microarray data, such as protein IDs and fold changes in individual probes. The 'common upstream' search algorithm aids in the extraction of the most relevant molecular network comprising genes that are coordinately regulated by putative common upstream transcription factors (23,24).

HSP90 inhibitors. In the *in vitro* experiments, 17-dimethylaminoethylamino-17-demethoxygeldanamycin (17-DMAG; AdooQ Bioscience) and ganetespib (KareBay Biochem, Inc.) were dissolved in DMSO to a stock concentration of 1 mM and the same final concentrations (5, 10 and 15 μM) were used, as previously described (25,26). The stock solutions were stored at -20˚C. The inhibitors were diluted in culture medium prior to each *in vitro* experiment, and 0.01% DMSO in culture medium was used as the vehicle control.

Cell proliferation assay. KON cells that strongly expressed the HSP90 protein were plated in 96-well plates (density, $5x10^3$ cells/well) in sextuplicate and incubated at 37˚C in a humidified 5% CO_2 atmosphere. Following an overnight attachment period, the cells were exposed to 17-DMAG (5, 10 and 15 μM), ganetespib (5, 10 and 15 μM) or 0.01% DMSO (as control) at 37˚C. The number of viable cells was counted after 24, 48 and 72 h using the RealTime-Glo MT Cell Viability Assay (Promega Corporation) and a GloMax 96 Microplate Luminometer (Promega Corporation) (27). All assays were performed with five technical replicates and each assay was repeated three times.

Cell invasion assay. The *in vitro* invasion assay was performed using the CultreCoat 96-well Basement Membrane Extract-Coated Invasion Assay Kit (Trevigen, Inc.) (28). The KON cells ($1x10^5$) suspended in serum-free culture medium were seeded on the upper surface of each insert chamber in triplicate. The lower part was filled with culture medium containing 10% FBS. The cells were exposed to 17-DMAG (5, 10 and 15 μM), ganetespib (5, 10 and 15 μM) or 0.01% DMSO at 37˚C for 48 h. Following incubation, the cells that had migrated to the other side of the membrane were detected using cell dissociation solution/calcein AM. The fluorescence was read using a 480/520 nm filter set.

Gap closure assay. KON cells were seeded on culture inserts ($3.0x10^5$ cells/insert; cat. no. 80206; Ibidi GmbH) in triplicate. When the cells reached confluency, the inserts were removed and a gap was created. After washing with PBS to remove the cell debris, the cells were exposed to 17-DMAG (5, 10 and 15 μM), ganetespib (5, 10 and 15 μM) or 0.01% DMSO, and incubated at 37˚C in a 5% CO_2 humidified incubator to allow for gap closure. The FBS concentration used in this experiment was 3% (29). The closure of the gap was imaged under a BZ-X710 microscope (light microscope; magnification, x40; Keyence Corporation) immediately after adding fresh culture medium and at the indicated time points (6, 12, 18, 24 and 30 h later) (27,30). The area of the gap at each time point was calculated using the MRI Wound healing tool (http://dev.mri.cnrs.fr/projects/imagej-macros/wiki/Wound_Healing_Tool) in ImageJ software (ver. 1.50; National Institutes of Health).

Western blot analysis. Western blotting was performed as previously described (27,30). The KON cells were seeded on culture plates (10x10 mm^2). At 60-70% confluency, they were treated with 17-DMAG (5, 10 and 15 μM), ganetespib (5, 10 and 15 μM) or 0.01% DMSO for 48 h. Proteins were extracted using the Mammalian Protein Extraction Reagent (Thermo Fisher Scientific, Inc.) containing a protease inhibitor mixture (FUJIFILM Wako Pure Chemical Corporation), Phosphatase Inhibitor Cocktail 2 (Sigma-Aldrich; Merck KGaA) and Phosphatase Inhibitor Cocktail 3 (Sigma-Aldrich; Merck KGaA) at a ratio of 1:100. The protein samples were fractionated by SDS-PAGE and blotted onto polyvinylidene difluoride membranes (Merck KGaA). The membranes were blocked with 5% PhosphoBLOCKE powder (Cell Biolabs, Inc.) in Tris-buffered saline and 1% Tween-20, and probed using the following antibodies: EGF receptor rabbit monoclonal antibody (dilution, 1:1,000; cat. no. 4267; Cell Signaling Technology, Inc.), phospho-EGF receptor rabbit monoclonal antibody (dilution, 1:1,000; cat. no. 3777; Cell Signaling Technology, Inc.), MEK1/2 rabbit monoclonal antibody (dilution, 1:1,000; cat. no. 8727; Cell Signaling Technology, Inc.), phospho-MEK1/2 rabbit monoclonal antibody (dilution, 1:1,000; cat. no. 9154; Cell Signaling Technology, Inc.), p44/42 MAPK rabbit polyclonal antibody (dilution, 1:1,000; cat. no. 9102; Cell Signaling Technology, Inc.), phospho-p44/42 MAPK rabbit monoclonal antibody (dilution, 1:2,000; cat. no. 4370; Cell Signaling Technology, Inc.), heat shock protein 70 (HSP70) rabbit polyclonal antibody (dilution, 1:1,000; cat. no. 4872; Cell Signaling Technology, Inc.), HSP90 rabbit monoclonal antibody (dilution, 1:1,000; cat. no. 4877; Cell Signaling Technology, Inc.) and β-actin mouse monoclonal antibody (dilution, 1:2,500; cat. no. ab6276; Abcam). Following overnight incubation with the primary antibodies at 4˚C, signals were detected using the relevant horseradish peroxidase-conjugated anti-mouse or anti-rabbit IgG antibodies (GE Healthcare) and the SuperSignal™ West Dura Extended Duration Substrate (Thermo Fisher Scientific, Inc.), according to the manufacturer's protocol. The levels of total and phosphorylated proteins were analyzed using the same protein sample. The experiments were performed in triplicate.

Tissue samples. Tumor tissues and patient-matched normal oral tissues (near the resection margin) were obtained at the time of surgical resection from Tokyo Dental College Chiba Hospital (Chiba, Japan) according to a protocol approved by the Institutional Review Board of Tokyo Dental College (approval no. 709). The inclusion criteria were: i) Having an OSCC of the tongue, ii) available formalin-fixed paraffin-embedded tumor samples; and iii) existence of essential clinical records corresponding to the tumor. The exclusion criteria were: i) Lack of essential survival data; ii) lack of sufficient quantity of tumor tissue in the paraffin block; and iii) microinvasive carcinomas or carcinoma in situ. Written informed consent was obtained from all patients involved. The subjects included 37 men and 21 women ranging in age between 30 and 86 years, with a mean age of 66 years, who underwent surgical excision between January 2009 and March 2014. The resected tissues were divided into two parts: One was frozen immediately and stored at -80˚C for further analyses and the other was fixed in 10% buffered formaldehyde solution for pathological diagnosis.

Table I. List of top 5 pathways contributing to the common upstream network identified by KeyMolnet.

Rank	Name	Score	Score(p)	Score(v)
1	HSP90 signaling pathway	47.28	$5.853x10^{-15}$	0.121
2	Transcriptional regulation by HIF	25.15	$2.683x10^{-8}$	0.053
3	Annexin signaling pathway	14.32	$4.870x10^{-5}$	0.030
4	PI3K signaling pathway	12.65	$1.550x10^{-4}$	0.038
5	Spliceosome assembly	12.13	$2.230x10^{-4}$	0.023

HIF, hypoxia-inducible factor; HSP90, heat shock protein 90.

Fixation was performed at room temperature for 24 h. The histopathological diagnosis of each tissue was performed according to the International Histological Classification of Tumors (31) at the Department of Pathology, Tokyo Dental College. Clinicopathological staging was conducted according to the TNM Classification of the International Union against Cancer (32).

IHC. IHC staining was performed as previously described (17,27). Paraffin-embedded specimens (4-μm-thick) were subjected to IHC staining. Briefly, following deparaffinization and hydration, the slides were treated with 0.3% H_2O_2 for 30 min to block endogenous peroxidase. Subsequently, the sections were blocked at room temperature for 2 h with 1.5% blocking serum (Santa Cruz Biotechnology, Inc.) in PBS and treated with the anti-HSP90 rabbit monoclonal antibody at a dilution of 1:1,000. The same primary antibodies were used for IHC and western blot analysis. Sections were incubated with the primary antibody in a moist chamber at room temperature for 30 min. Following incubation, the sections were washed three times in PBS and treated with Envision reagent (Dako; Agilent Technologies, Inc.), followed by color development in 3,3'-diaminobenzidine tetrahydrochloride (Dako; Agilent Technologies, Inc.). The slides were then lightly counterstained with hematoxylin and mounted. Duplicate sections immunostained without exposure to the primary antibodies served as negative controls. A scoring method was used to quantitate the protein expression levels of HSP90, with the mean percentage of positive tumor cells being assessed in at least five random fields (magnification, x400) in each section. The intensity of the HSP90 immunoreaction was scored as follows: 1+, weak; 2+, moderate; and 3+, intense. The percentage of positive tumor cells and staining intensity were multiplied to produce an HSP90-IHC staining score for each case (27,30). The IHC scores of the tumor tissues were compared with those of the healthy surrounding normal tissues obtained from the same patient. Cancer tissues with higher IHC scores than those of the adjacent normal tissues were designated as HSP90 high expression cases. The cases were scored by two independent specialists who were blinded to the clinical status of the patients.

Statistical analysis. The *in vitro* assay results were evaluated using Student's t-test and ANOVA with Bonferroni's correction applied. Data are presented as the mean ± SD. All assays were repeated three times. Significant differences between HSP90-IHC scores and clinicopathological features were assessed using the Mann-Whitney U test and Fisher's exact test. The overall survival rate was calculated by Kaplan-Meier analysis, and the log-rank test was used for comparisons between groups. Statistical analyses were performed using EZR, ver. 1.42 (Saitama Medical Center, Jichi Medical University, Saitama, Japan), which is a graphical user interface for R (The R Foundation) and a modified version of R Commander that adds statistical functions frequently used in biostatistics (27,33). All P-values were two-sided, and $P \leq 0.05$ was considered to indicate a statistically significant difference.

Results

Proteomic profiling by 2D-DIGE. OSCC-derived cell lines and HaCaT cells were subjected to protein extraction. From each proteome, ~3,000 protein spots were successfully identified (Fig. 1A). The expression levels of 49 proteins were significantly increased and those of 77 proteins were significantly decreased in the OSCC cells compared with in the HaCaT cells. LC-MS/MS identified 92 types of proteins, except those with post-translational modifications (Fig. 1B).

Hierarchical clustering and partition analyses of samples. Fig. 1B shows the results obtained in the clustering analysis. Samples with high expression levels are shown in green, and those with low expression levels in red. The columns indicate the samples, whereas the rows indicate the proteins. The dendrograms represent the distances between the clusters. To identify relationships between the molecular network of the OSCC cells and the canonical pathway, an 'interrelation' network search was performed using the KeyMolnet® software. A common upstream search was performed using this software for proteins with expression abnormalities that were identified in the proteomic analysis of OSCC cells. In the extracted molecular network, the five pathways with the highest scores were the 'HSP90 signaling pathway' (score, 47.28), 'transcriptional regulation by HIF' (score, 25.15), 'Annexin signaling pathway' (score, 14.32), 'PI3K signaling pathway' (score, 12.65) and 'Spliceosome assembly' (score, 12.13; Table I). The results obtained revealed HSP90 as a target which regulates the functional maintenance and stability of numerous client proteins that serve roles in OSCC cell proliferation and survival. A typical network including HSP90 (Table I; rank 1) is shown in Fig. 1C. HSP90 was listed as a candidate protein that frequently exhibited high expression levels in OSCC cell lines (Fig. 2A and B).

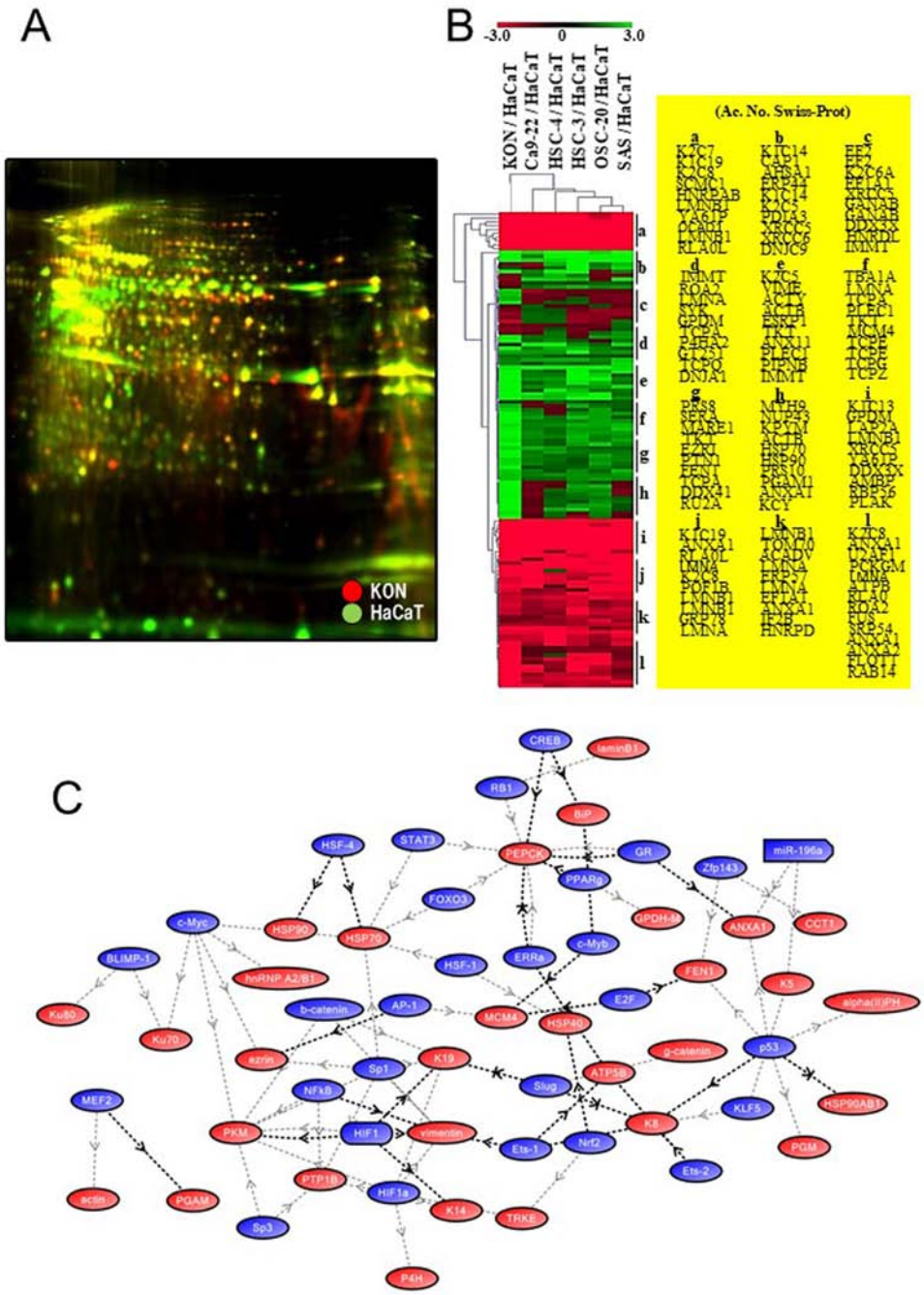

Figure 1. Comparative analysis of OSCC-derived cells (KON) and HaCaT cells using the 2D-DIGE system. (A) Typical 2D-DIGE gel image of OSCC-derived cells and HaCaT cells. Protein lysates were labeled with Cy3 (green; HaCaT cells) or Cy5 (red; KON cells) and subjected to 2D-DIGE. (B) Expression profile analysis of OSCC-derived cells and HaCaT cells. Hierarchical cluster analysis of the expression profiles of 92 types of proteins. The most intense green blocks represent strongly upregulated proteins and the most intense red blocks show proteins with the greatest degree of downregulation. (C) Molecular network of OSCC-related proteins. A common upstream search was performed using the KeyMolnet® software for proteins with expression abnormalities that were found in a proteomic analysis of OSCC cells. A typical network including HSP90 is shown. As a result of the proteomic analysis, a molecule in which an expression variation was observed is shown with a red background, and other molecules are shown with blue backgrounds. The molecules are linked with black arrows when the studies that provided the basis of linkage were review articles, and with gray arrows when the studies were original articles. 2D-DIGE, two-dimensional fluorescence difference gel electrophoresis; Ac. No., accession number; HSP90, heat shock protein 90; OSCC, oral squamous cell carcinoma.

17-DMAG and ganetespib decrease cell viability and invasion in OSCC-derived cell lines in vitro. The HSP90 inhibitors 17-DMAG and ganetespib were selected for *in vitro* validation as potential therapeutic target molecules for OSCC. HSP90 was more highly expressed in KON cells than in the other OSCC-derived cell lines. Therefore, this cell line was examined in subsequent assays. The viability of cells treated with increasing concentrations of 17-DMAG or ganetespib for 24, 48 and 72 h was assessed using the MT Cell Viability Assay. As shown in Fig. 3A, the viability of KON cells treated with 17-DMAG or ganetespib was significantly reduced within 24 h of treatment ($P<0.05$). To clarify the effects of 17-DMAG or ganetespib on the invasive ability of the cells, the KON cell lines were treated with 17-DMAG (5, 10 and 15 μM),

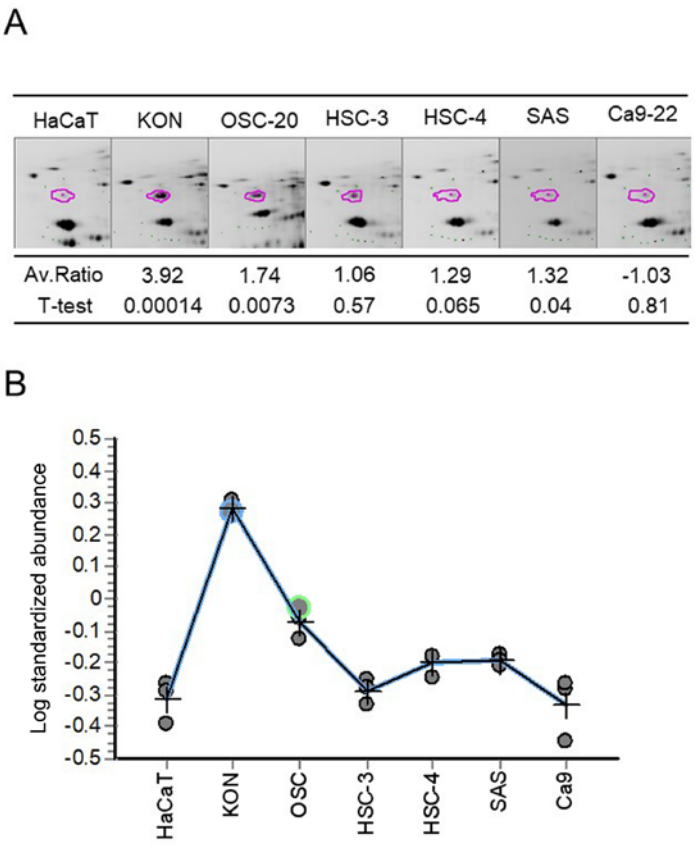

Figure 2. HSP90 expression in HaCaT and OSCC cell lines. (A) HSP90 electrophoretic patterns in each cell line. (B) HSP90 protein was more strongly expressed in most OSCC cell lines compared with in the HaCaT cells. HSP90, heat shock protein 90; OSCC, oral squamous cell carcinoma.

ganetespib (5, 10 and 15 μM) or 0.01% DMSO for 48 h. The results obtained revealed significantly lower invasion rates in treated cells compared with the untreated cells (Fig. 3B). The gap closure assay investigated gap closure in KON cells 30 h after the DMSO treatment. Additional cells were observed in the vicinity of the gap. By contrast, gap closure was slower in HSP90 inhibitor-treated KON cells (Fig. 3C and D). This difference in gap closure was statistically significant at 18, 24 and 30 h ($P<0.05$).

17-DMAG and ganetespib alter the in vitro expression levels of HSP90-related proteins in OSCC cells. In an attempt to clarify the *in vitro* effects of 17-DMAG and ganetespib in the OSCC-derived cell lines, the expression levels of HSP90 and its related proteins were assessed by western blot analysis. The cells were exposed to 17-DMAG (5, 10 and 15 μM), ganetespib (5, 10 and 15 μM) or DMSO for 48 h, lysed and then subjected to western blotting using commercial antibodies. As shown in Fig. 4, the expression levels of HSP90, HSP70, MEK and MAPK were increased in the HSP90 inhibitor-treated KON cells, whereas those of the HSP90 target proteins EGFR, phospho-EGFR, phospho-MEK and phospho-MAPK were decreased in the 17-DMAG- and ganetespib-treated cells.

HSP90 protein expression in normal oral tissues and primary OSCCs. Twenty-six out of the 58 OSCC samples subjected to IHC staining exhibited increased expression levels of HSP90. By contrast, normal tissues exhibited weak cytoplasmic immunoreactions for HSP90. Fig. 5A-C shows representative results for HSP90 protein expression in normal oral tissue and primary OSCCs. A significant association between high HSP90 expression and regional lymph node metastasis was noted (Table II). The protein expression levels of HSP90 in normal oral tissue and primary OSCC samples are shown in Fig. 5D. The HSP90-IHC scores ranged between 2.89 and 165.98 (mean, 75.66), 31.37 and 258.77 (mean, 104.39), 31.37 and 165.45 (mean, 79.53), and 63.81 and 258.77 (mean, 146.54) in the normal tissues, OSCC samples, and the node-negative (pN-) and node-positive (pN+) OSCC samples, respectively. Significant differences in HSP90-IHC scores between the normal oral tissues and OSCC samples were observed ($P=0.005$; Fig. 5D). Furthermore, the expression levels of HSP90 were significantly higher ($P=0.015$) in the pN^+ OSCC samples compared with the pN^- OSCC samples. The results of the Kaplan-Meier analysis revealed that, based on the overall survival rates of 58 patients, high expression levels of HSP90 were not associated with poor outcomes ($P=0.606$; Fig. 5E).

Discussion

Proteome analysis, which is the study of protein complements in a cell, has the potential to accurately identify proteins that can be used as novel targets during therapeutic interventions and biomarkers for early cancer detection (34,35). The establishment of effective cancer therapeutics based on the inhibition of a protein that regulates numerous signaling pathways and shows abnormalities in cancer cells is an attractive approach

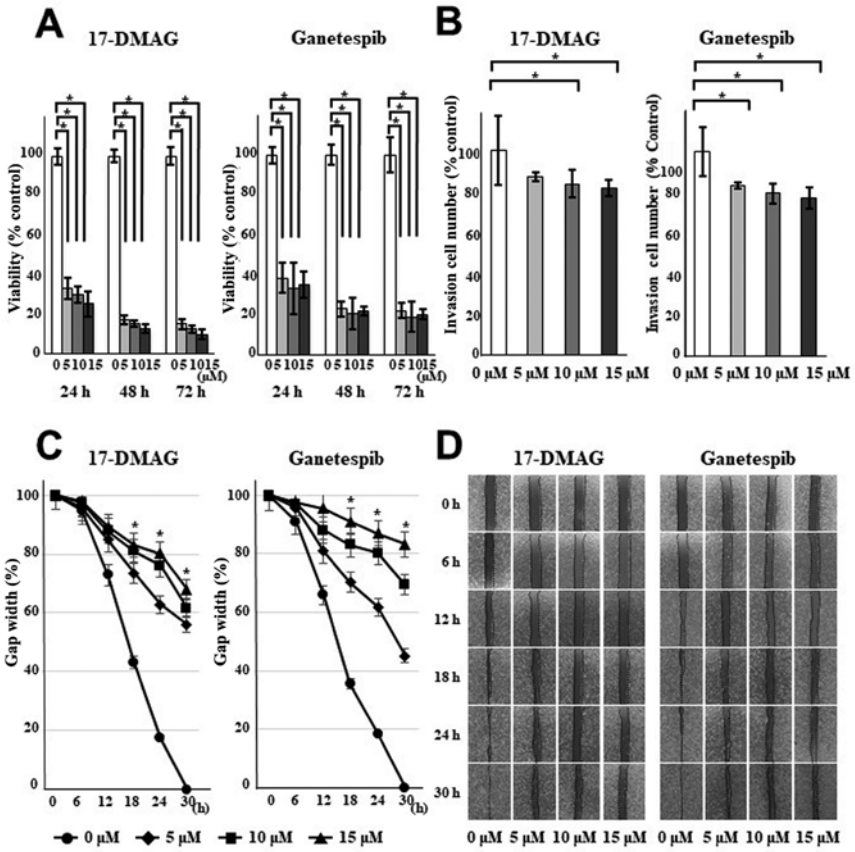

Figure 3. *In vitro* effects of 17-DMAG and ganetespib on cell proliferation and migration in OSCC-derived cell lines. (A) KON cells were treated with increasing concentrations of 17-DMAG and ganetespib. Cell viability was assessed after 24, 48 and 72 h of treatment. Data are presented as the mean ± SD of at least three independent experiments in quintuplicate. *P<0.05. (B) Cell invasion was evaluated in KON cells treated with 17-DMAG or ganetespib (5, 10 and 15 μM) for 48 h. DMSO-treated KON cells were used as the control. Data are presented as the mean ± SD. *P<0.05 (t-test and ANOVA with Bonferroni's correction). (C) Gap closure assay after treatment with the HSP90 inhibitor. After uniform gaps were created in confluent cultures of 17-DMAG-, ganetespib- and DMSO-treated KON cells, the extent of closure was visually monitored. The gap was completely sealed after 30 h in the DMSO-treated control cells, but remained open in the HSP90 inhibitor-treated cells. *P<0.05 vs. 0 μM (t-test and ANOVA with Bonferroni's correction). (D) Widths of the gaps were measured at predefined positions and specific time points. Magnification, x40. The migration of HSP90 inhibitor-treated cells was decreased compared with that of the control cells at 18, 24 and 30 h after the creation of the gaps. 17-DMAG, 17-dimethylaminoethylamino-17-demethoxygeldanamycin; HSP90, heat shock protein 90; OSCC, oral squamous cell carcinoma.

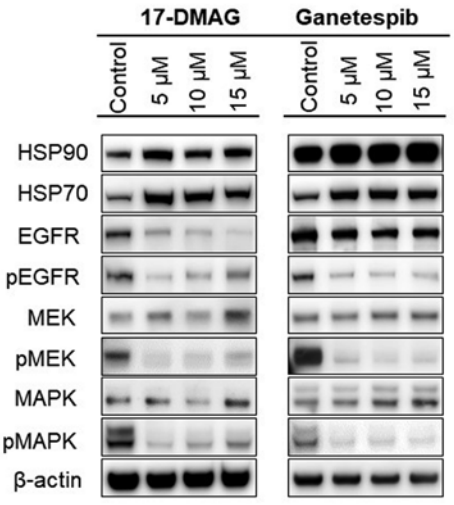

Figure 4. *In vitro* effects of 17-DMAG and ganetespib on HSP90 and HSP90-associated protein expression in KON cells treated with various concentrations (5, 10 and 15 μM) of 17-DMAG or ganetespib for 48 h. DMSO-treated KON cells were used as the control. Western blot analysis was performed using antibodies against HSP90 and HSP90-associated proteins. Protein loading was normalized using an antibody that recognized β-actin. 17-DMAG, 17-dimethylaminoethylamino-17-demethoxygeldanamycin; HSP70, heat shock protein 70; HSP90, heat shock protein 90; p, phosphorylated.

for cancer therapy (36). A common upstream search was performed using the protein nucleic acid database for proteins with expression abnormalities that were identified following a proteomic analysis of OSCC cells. HSP90 was identified as a potentially novel molecular marker and target, which regulates the functional maintenance and stability of numerous client proteins that are involved in the proliferation and survival of OSCC cells. Previous studies of proteomic analysis of OSCC tissues also reported abnormal protein expression levels of HSP90 (37,38). HSP90 has emerged as a novel therapeutic target that simultaneously regulates numerous oncogenic client proteins, which are the pathological hallmarks of malignancy (39). HSP90 functions as a chaperone protein in the stabilization and conformational maturation of a large number of oncoproteins (11). HSP90 has been implicated in the pathogenesis, poor prognosis and resistance to therapy of various types of cancer in humans (40,41). Furthermore, HSP90 target proteins are involved in most aspects of the oncogenic process, such as immortality, survival, anti-apoptosis, genomic instability, neoangiogenesis and metastasis (42,43). In a previous study, blocking of ATP-binding sites on the HSP90-partner complex resulted in the dephosphorylation and/or proteasomal degradation of these target proteins, thus demonstrating a

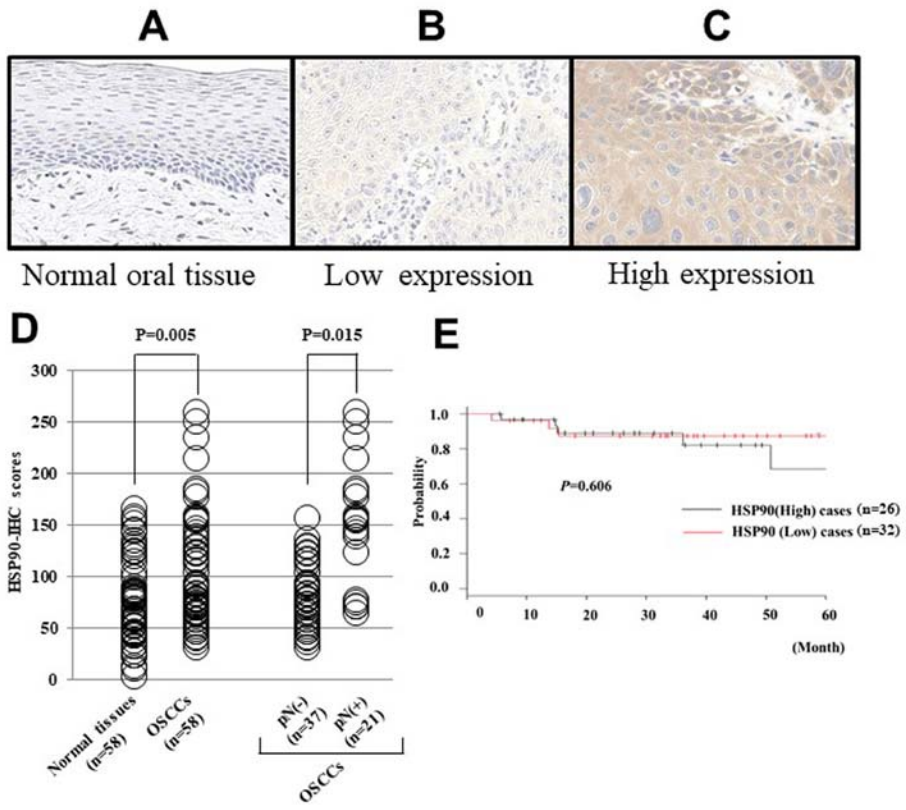

Figure 5. Immunohistochemistry scores of HSP90 in normal and tumorous oral tissues. (A) Normal oral tissue expressed the HSP90 protein, which was limited to the cytoplasm of the epithelial cells. (B) A primary OSCC case with low HSP90 expression. (C) A primary OSCC case with high HSP90 expression. Original magnification, x400. (D) A significant difference was observed in HSP90 protein expression between the pN(-) and pN(+) OSCC cases (P=0.015; Fisher's exact test). (E) Kaplan-Meier survival analysis. No significant differences were noted in survival rates between the HSP90-high and HSP90-low expression groups (P=0.606). HSP90, heat shock protein 90; OSCC, oral squamous cell carcinoma; pN(-), node-negative; pN(+), node-positive.

potent antitumor activity (44). Among the various HSP90 inhibitors currently available, geldanamycin (GA), a benzoquinone ansamycin compound, belongs to the originally identified benzoquinone class of compounds. GA derivatives, such as the less toxic 17-allylamino-17-demethoxygeldanamycin (17-AAG) and 17-DMAG, have been developed. 17-DMAG is water-soluble and, therefore, orally available (45,46). Furthermore, it has numerous advantages over 17-AAG, such as less hepatotoxicity, high potency, less extensive metabolism and a longer plasma half-time (45,46). A phase I trial of 17-DMAG validated its clinical usefulness in various types of cancer, including acute myeloid leukemia (partial response), castration-refractory prostate cancer (complete response), melanoma (partial response), renal cancer (stable disease) and chondrosarcoma (stable disease) (47). However, to the best of our knowledge, this was the first study to examine its effect in oral cancer.

Ganetespib (previously referred to as STA-9090), a second-generation HSP90 inhibitor, is cytotoxic *in vitro* and exhibits antitumor activity against a wide range of cancer types with promising safety profiles *in vivo* (48,49). Previous clinical trials have reported the promising effects of this agent against human breast and lung cancer (50,51). A few studies on HSP90 suppression using 17-AAG in OSCC have been published (52,53). However, to the best of our knowledge, the anticancer effects of 17-DMAG and ganetespib against OSCC have not yet been examined in detail.

Similar to previous findings obtained in other tumor cells treated with HSP90 inhibitors (25,51), the present results demonstrated that cell viability and migration were reduced in OSCC cells treated with 17-DMAG and ganetespib. These effects were associated with markedly decreased expression levels of target proteins of HSP90, including EGFR, phospho-EGFR, phospho-MEK and phospho-MAPK. Furthermore, in concordance with the findings of other studies (54,55), a marked increase in the expression levels of HSP90 and HSP70 following 17-DMAG and ganetespib treatment was observed in the present study, probably through the activation of the heat shock transcription factor 1 (HSF1), which is a master stress-inducible regulator in the cytoplasm and the nucleus (56,57), or due to the disruption of the nuclear HSP90/multichaperone complexes that inhibit the activation of DNA-bound HSF1 (58). The majority of the HSP90 inhibitors activate HSF1 and induce survival factors, such as HSP70, indicating that HSF1 is one of the client proteins of HSP90. Normally, HSF1 binds to the chaperone complex, which consists of HSP90 and remains in an inactive state. In other words, HSP90 negatively regulates HSF1 activity. Therefore, when the function of HSP90 is suppressed by an inhibitor, HSF1 is released and activated leading to the induction of several HSPs, thus making the cells stress-resistant. This offsets the cytocidal effect of HSP90 inhibitors (56-58). Additionally, the induction of HSP70 is an indicator of the presence of HSP90 inhibitors (56-58). The induction of HSP70 by an HSP90

Table II. Association between the expression levels of HSP90 and clinical classification in patients with oral squamous cell carcinoma (n=58).

Clinical classification	No. of patients (n=58)	HSP90 expression		P-value
		Low, n (%)	High, n (%)	
Age at surgery, years				
<60	22	14 (64)	8 (36)	0.67
≥60, <70	18	9 (50)	9 (50)	
≥70	18	9 (50)	9 (50)	
Sex				
Male	37	20 (54)	17 (46)	1
Female	21	12 (57)	9 (43)	
T-primary tumor				
T1	16	8 (50)	8 (50)	0.897
T2	20	11 (55)	9 (45)	
T3	6	3 (50)	3 (50)	
T4	16	10 (63)	6 (37)	
N-regional lymph node				
pN(+)	21	7 (33)	14 (67)	0.015
pN(-)	37	25 (68)	12 (32)	
Stage				
I	16	8 (50)	8 (50)	0.709
II	17	8 (47)	9 (53)	
III	9	6 (67)	3 (33)	
IV	16	10 (63)	6 (37)	
I, II	33	16 (48)	17 (52)	0.292
III, IV	25	16 (64)	9 (36)	
Histological type				
Well differentiated	46	25 (54)	21 (46)	0.444
Moderately differentiated	7	3 (43)	4 (57)	
Poorly differentiated	5	4 (80)	1 (20)	

HSP90, heat shock protein 90; pN(-), node-negative; pN(+), node-positive.

inhibitor may enhance the antitumor effects when combined with other inhibitors, such as an HSP70 inhibitor, or radiation. Musha *et al* (59) previously examined the effects of 17-AAG in combination with X-rays or carbon ion beams on OSCC cells and reported that it exerted synergistic effects on cell lethality with X-rays, but not with carbon ion beams. Further studies are required to investigate the synergistic effects of 17-DMAG or ganetespib with X-rays or carbon ion beams.

In the present study, the HSP90 expression status based on IHC scores in the clinical tissue samples obtained from primary OSCC and corresponding normal oral tissues revealed high frequencies of HSP90-high cases. Furthermore, associations were noted between the HSP90 expression status and clinicopathological features. Although most primary OSCC samples with HSP90-high expression presented with regional lymph node metastasis, tumors without metastatic lesions had low HSP90 expression levels (P=0.015). These results are consistent with previous findings reported by Chang *et al* (60), which revealed high HSP90 protein expression in 36 OSCC cases, and an association between HSP90-high expression cases and lymph node metastasis. However, unlike the findings of a previous study, which reported a lower survival rate in patients with high HSP90 expression levels (60,61), no such relationship was observed in the present study. The study by Chang *et al* (60) comprised only 36 cases, whereas the cases reported by Ono *et al* (61) had an extremely poor 5-year survival rate compared with those in the present study. These differences may have influenced the results of the present study.

One of the limitations of the present study was the small sample size, which may have affected the results. On the other hand, the *in vitro* analysis verified the effect of HSP90 inhibitors on only one KON cell line that expressed HSP90 protein at the highest level. Analyzing the effects of HSP90 inhibitors on a number of other types of OSCC cell lines is a future challenge. Nonetheless, to the best of our knowledge, the present study was the first to demonstrate the effects of 17-DMAG and ganetespib in OSCC. OSCC cells treated with 17-DMAG

and ganetespib exhibited reduced cell viability and migration, which were associated with markedly decreased expression levels of the HSP90 target proteins EGFR, phospho-EGFR, phospho-MEK and phospho-MAPK. Therefore, the present results indicate the potential of HSP90 as a novel target for the early detection, prevention and treatment of oral cancer metastasis. It was speculated that the suppression of HSP90 may prevent metastasis associated with oral carcinogenesis, while the upregulated expression levels of HSP90 in primary OSCC may promote invasiveness, motility and metastasis. Further studies with a large sample size will contribute to the development of strategies for the diagnosis, prevention and treatment of this neoplasm.

Acknowledgements

Not applicable.

Funding

The present study was supported by JSPS KAKENHI (grant no. 16K11701 and 19K10366).

Availability of data and materials

The datasets used and/or analyzed during the current study are available from the corresponding author on reasonable request.

Authors' contributions

NS, TO and TS were involved in the conception and design of the present study. NS and TO performed experiments, analyzed data and drafted the manuscript. KH, KO, KW and SS interpreted the data and assisted in manuscript preparation. All authors read and approved the final manuscript.

Ethics approval and consent to participate

The present study was approved by the Research Ethics Committee of Tokyo Dental College (approval no. 709), and written informed consent was obtained from all patients involved.

Patient consent for publication

Not applicable.

Competing interests

The authors declare that they have no competing interests.

References

1. Siegel R, Ma J, Zou Z and Jemal A: Cancer statistics, 2014. CA Cancer J Clin 64: 9-29, 2014.
2. Prestwich R, Dyker K and Sen M: Improving the therapeutic ratio in head and neck cancer. Lancet Oncol 11: 512-513, 2010.
3. Stransky N, Egloff AM, Tward AD, Kostic AD, Cibulskis K, Sivachenko A, Kryukov GV, Lawrence MS, Sougnez C, McKenna A, *et al*: The mutational landscape of head and neck squamous cell carcinoma. Science 333: 1157-1160, 2011.
4. Srinivas PR, Verma M, Zhao Y and Srivastava S: Proteomics for cancer biomarker discovery. Clin Chem 48: 1160-1169, 2002.
5. Dabbous MK, Jefferson MM, Haney L and Thomas EL: Biomarkers of metastatic potential in cultured adenocarcinoma clones. Clin Exp Metastasis 28: 101-111, 2011.
6. Poli G, Ceni E, Armignacco R, Ercolino T, Canu L, Baroni G, Nesi G, Galli A, Mannelli M and Luconi M: 2D-DIGE proteomic analysis identifies new potential therapeutic targets for adrenocortical carcinoma. Oncotarget 6: 5695-5706, 2015.
7. Merkley MA, Weinberger PM, Jackson LL, Podolsky RH, Lee JR and Dynan WS: 2D-DIGE proteomic characterization of head and neck squamous cell carcinoma. Otolaryngol Head Neck Surg 141: 626-632, 2009.
8. Bijian K, Mlynarek AM, Balys RL, Jie S, Xu Y, Hier MP, Black MJ, Di Falco MR, LaBoissiere S and Alaoui-Jamali MA: Serum proteomic approach for the identification of serum biomarkers contributed by oral squamous cell carcinoma and host tissue microenvironment. J Proteome Res 8: 2173-2185, 2009.
9. Whitesell L and Lindquist SL: HSP90 and the chaperoning of cancer. Nat Rev Cancer 5: 761-772, 2005.
10. Solit DB and Rosen N: Hsp90: A novel target for cancer therapy. Curr Top Med Chem 6: 1205-1214, 2006.
11. Trepel J, Mollapour M, Giaccone G and Neckers L: Targeting the dynamic HSP90 complex in cancer. Nat Rev Cancer 10: 537-549, 2010.
12. Taldone T, Gozman A, Maharaj R and Chiosis G: Targeting Hsp90: Small-molecule inhibitors and their clinical development. Curr Opin Pharmacol 8: 370-374, 2008.
13. Neckers L and Workman P: Hsp90 molecular chaperone inhibitors: Are we there yet? Clin Cancer Res 18: 64-76, 2012.
14. Zhao M, Sano D, Pickering CR, Jasser SA, Henderson YC, Clayman GL, Sturgis EM, Ow TJ, Lotan R, Carey TE, *et al*: Assembly and initial characterization of a panel of 85 genomically validated cell lines from diverse head and neck tumor sites. Clin Cancer Res 17: 7248-7264, 2011.
15. Yu M, Selvaraj SK, Liang-Chu MM, Aghajani S, Busse M, Yuan J, Lee G, Peale F, Klijn C, Bourgon R, *et al*: A resource for cell line authentication, annotation and quality control. Nature 520: 307-311, 2015.
16. Koike H, Uzawa K, Nakashima D, Shimada K, Kato Y, Higo M, Kouzu Y, Endo Y, Kasamatsu A and Tanzawa H: Identification of differentially expressed proteins in oral squamous cell carcinoma using a global proteomic approach. Int J Oncol 27: 59-67, 2005.
17. Onda T, Uzawa K, Nakashima D, Saito K, Iwadate Y, Seki N, Shibahara T and Tanzawa H: Lin-7C/VELI3/MALS-3: An essential component in metastasis of human squamous cell carcinoma. Cancer Res 67: 9643-9648, 2007.
18. Nishikawa H, Ooka S, Sato K, Arima K, Okamoto J, Klevit RE, Fukuda M and Ohta T: Mass spectrometric and mutational analyses reveal Lys-6-linked polyubiquitin chains catalyzed by BRCA1-BARD1 ubiquitin ligase. J Biol Chem 279: 3916-3924, 2004.
19. Dyrlund TF, Poulsen ET, Scavenius C, Sanggaard KW and Enghild JJ: MS Data Miner: A web-based software tool to analyze, compare, and share mass spectrometry protein identifications. Proteomics 12: 2792-2796, 2012.
20. Hao P, Ren Y, Tam JP and Sze SK: Correction of errors in tandem mass spectrum extraction enhances phosphopeptide identification. J Proteome Res 12: 5548-5557, 2013.
21. Yadav R and Srivastava P: Clustering, Pathway Enrichment, and Protein-Protein Interaction Analysis of Gene Expression in Neurodevelopmental Disorders. Adv Pharmacol Sci 2018: 3632159, 2018.
22. Lu J, Tao YF, Li ZH, Cao L, Hu SY, Wang NN, Du XJ, Sun LC, Zhao WL, Xiao PF, *et al*: Analyzing the gene expression profile of anaplastic histology Wilms' tumor with real-time polymerase chain reaction arrays. Cancer Cell Int 15: 44, 2015.
23. Sato H, Ishida S, Toda K, Matsuda R, Hayashi Y, Shigetaka M, Fukuda M, Wakamatsu Y and Itai A: New approaches to mechanism analysis for drug discovery using DNA microarray data combined with KeyMolnet. Curr Drug Discov Technol 2: 89-98, 2005.
24. Satoh J, Tabunoki H and Arima K: Molecular network analysis suggests aberrant CREB-mediated gene regulation in the Alzheimer disease hippocampus. Dis Markers 27: 239-252, 2009.
25. Weber H, Valbuena JR, Barbhuiya MA, Stein S, Kunkel H, García P, Bizama C, Riquelme I, Espinoza JA, Kurtz SE, *et al*: Small molecule inhibitor screening identifified HSP90 inhibitor 17-AAG as potential therapeutic agent for gallbladder cancer. Oncotarget 8: 26169-26184, 2017.

26. Klameth L, Rath B and Hamilton G: In vitro Cytotoxic Activities of the Oral Platinum(IV) Prodrug Oxoplatin and HSP90 Inhibitor Ganetespib against a Panel of Gastric Cancer Cell Lines. J Cancer 8: 1733-1743, 2017.
27. Sekikawa S, Onda T, Miura N, Nomura T, Takano N, Shibahara T and Honda K: Underexpression of α-1-microglobulin/bikunin precursor predicts a poor prognosis in oral squamous cell carcinoma. Int J Oncol 53: 2605-2614, 2018.
28. Islam F, Gopalan V, Law S, Tang JC and Lam AK: FAM134B promotes esophageal squamous cell carcinoma in vitro and its correlations with clinicopathologic features. Hum Pathol 87: 1-10, 2019.
29. Tricarico PM, Zupin L, Ottaviani G, Pacor S, Jean-Louis F, Boniotto M and Crovella S: Photobiomodulation therapy promotes in vitro wound healing in nicastrin KO HaCaT cells. J Biophotonics 11: e201800174, 2018.
30. Ogane S, Onda T, Takano N, Yajima T, Uchiyama T and Shibahara T: Spleen tyrosine kinase as a novel candidate tumor suppressor gene for human oral squamous cell carcinoma. Int J Cancer 124: 2651-2657, 2009.
31. Pindborg JJ, Reichart PA, Smith CJ and Waal IV: Histological typing of cancer and precancer of the oral mucosa. In: International Histological Classification of Tumours. 2nd edition. World Health Organization, Geneva, pp1-83, 1997.
32. Sobin LH, Gospodarowicz MK and Wittekind CH (eds.): TNM Classification of Malignant Tumours. 7th edition. Wiley-Blackwell, Singapore, pp22-58, 2009.
33. Kanda Y: Investigation of the freely available easy-to-use software 'EZR' for medical statistics. Bone Marrow Transplant 48: 452-458, 2013.
34. Herrmann PC, Liotta LA and Petricoin EF III: Cancer proteomics: The state of the art. Dis Markers 17: 49-57, 2001.
35. Johann DJ Jr, McGuigan MD, Patel AR, Tomov S, Ross S, Conrads TP, Veenstra TD, Fishman DA, Whiteley GR, Petricoin EF III, *et al*: Clinical proteomics and biomarker discovery. Ann N Y Acad Sci 1022: 295-305, 2004.
36. Zhang T, Hamza A, Cao X, Wang B, Yu S, Zhan CG and Sun D: A novel Hsp90 inhibitor to disrupt Hsp90/Cdc37 complex against pancreatic cancer cells. Mol Cancer Ther 7: 162-170, 2008.
37. Thiel UJ, Feltens R, Adryan B, Gieringer R, Brochhausen C, Schuon R, Fillies T, Grus F, Mann WJ and Brieger J: Analysis of differentially expressed proteins in oral squamous cell carcinoma by MALDI-TOF MS. J Oral Pathol Med 40: 369-379, 2011.
38. Chanthammachat P, Promwikorn W, Pruegsanusak K, Roytrakul S, Srisomsap C, Chokchaichamnankit D, Svasti J, Boonyaphiphat P, Singkhamanan K and Thongsuksai P: Comparative proteomic analysis of oral squamous cell carcinoma and adjacent non-tumour tissue from Thailand. Arch Oral Biol 58: 1677-1685, 2013.
39. Workman P, Burrows F, Neckers L and Rosen N: Drugging the cancer chaperone HSP90: Combinatorial therapeutic exploitation of oncogene addiction and tumor stress. Ann N Y Acad Sci 1113: 202-216, 2007.
40. McCarthy MM, Pick E, Kluger Y, Gould-Rothberg B, Lazova R, Camp RL, Rimm DL and Kluger HM: HSP90 as a marker of progression in melanoma. Ann Oncol 19: 590-594, 2008.
41. Lin P, Yi Y, Lu M, Wang M, Yang Y, Lu Y, Song S, Zheng Z, Deng X and Zhang L: Heat shock protein 90 inhibitor myco-epoxydiene modulates kinase signaling in cervical cancer cells and inhibits in-vivo tumor growth. Anticancer Drugs 26: 25-34, 2015.
42. Kaplan KB and Li R: A prescription for 'stress' - the role of Hsp90 in genome stability and cellular adaptation. Trends Cell Biol 22: 576-583, 2012.
43. Azoitei N, Diepold K, Brunner C, Rouhi A, Genze F, Becher A, Kestler H, van Lint J, Chiosis G, Koren J III, *et al*: HSP90 supports tumor growth and angiogenesis through PRKD2 protein stabilization. Cancer Res 74: 7125-7136, 2014.
44. Kamal A and Burrows FJ: Hsp90 inhibitors as selective anti-cancer drugs. Discov Med 4: 277-280, 2004.
45. Jhaveri K, Miller K, Rosen L, Schneider B, Chap L, Hannah A, Zhong Z, Ma W, Hudis C and Modi S: A phase I dose-escalation trial of trastuzumab and alvespimycin hydrochloride (KOS-1022; 17 DMAG) in the treatment of advanced solid tumors. Clin Cancer Res 18: 5090-5098, 2012.
46. Eiseman JL, Lan J, Lagattuta TF, Hamburger DR, Joseph E, Covey JM and Egorin MJ: Pharmacokinetics and pharmacodynamics of 17-demethoxy 17-[[(2-dimethylamino)ethyl]amino] geldanamycin (17DMAG, NSC 707545) in C.B-17 SCID mice bearing MDA-MB-231 human breast cancer xenografts. Cancer Chemother Pharmacol 55: 21-32, 2005.
47. Pacey S, Wilson RH, Walton M, Eatock MM, Hardcastle A, Zetterlund A, Arkenau HT, Moreno-Farre J, Banerji U, Roels B, *et al*: A phase I study of the heat shock protein 90 inhibitor alvespimycin (17-DMAG) given intravenously to patients with advanced solid tumors. Clin Cancer Res 17: 1561-1570, 2011.
48. Liu H, Xiao F, Serebriiskii IG, O'Brien SW, Maglaty MA, Astsaturov I, Litwin S, Martin LP, Proia DA, Golemis EA, *et al*: Network analysis identifies an HSP90-central hub susceptible in ovarian cancer. Clin Cancer Res 19: 5053-5067, 2013.
49. Proia DA, Zhang C, Sequeira M, Jimenez JP, He S, Spector N, Shapiro GI, Tolaney S, Nagai M, Acquaviva J, *et al*: Preclinical activity profile and therapeutic efficacy of the HSP90 inhibitor ganetespib in triple-negative breast cancer. Clin Cancer Res 20: 413-424, 2014.
50. Socinski MA, Goldman J, El-Hariry I, Koczywas M, Vukovic V, Horn L, Paschold E, Salgia R, West H, Sequist LV, *et al*: A multicenter phase II study of ganetespib monotherapy in patients with genotypically defined advanced non-small cell lung cancer. Clin Cancer Res 19: 3068-3077, 2013.
51. Powers MV, Valenti M, Miranda S, Maloney A, Eccles SA, Thomas G, Clarke PA and Workman P: Mode of cell death induced by the HSP90 inhibitor 17-AAG (tanespimycin) is dependent on the expression of pro-apoptotic BAX. Oncotarget 4: 1963-1975, 2013.
52. Hadley KE and Hendricks DT: Use of NQO1 status as a selective biomarker for oesophageal squamous cell carcinomas with greater sensitivity to 17-AAG. BMC Cancer 14: 334, 2014.
53. Shintani S, Zhang T, Aslam A, Sebastian K, Yoshimura T and Hamakawa H: P53-dependent radiosensitizing effects of Hsp90 inhibitor 17-allylamino-17-demethoxygeldanamycin on human oral squamous cell carcinoma cell lines. Int J Oncol 29: 1111-1117, 2006.
54. Lin SF, Lin JD, Hsueh C, Chou TC, Yeh CN, Chen MH and Wong RJ: Efficacy of an HSP90 inhibitor, ganetespib, in preclinical thyroid cancer models. Oncotarget 8: 41294-41304, 2017.
55. Ghadban T, Jessen A, Reeh M, Dibbern JL, Mahner S, Mueller V, Wellner UF, Güngör C, Izbicki JR and Vashist YK: In vitro study comparing the efficacy of the water-soluble HSP90 inhibitors, 17-AEPGA and 17-DMAG, with that of the non water-soluble HSP90 inhibitor, 17-AAG, in breast cancer cell lines. Int J Mol Med 38: 1296-1302, 2016.
56. Westerheide SD and Morimoto RI: Heat shock response modulators as therapeutic tools for diseases of protein conformation. J Biol Chem 280: 33097-33100, 2005.
57. Bagatell R, Paine-Murrieta GD, Taylor CW, Pulcini EJ, Akinaga S, Benjamin IJ and Whitesell L: Induction of a heat shock factor 1-dependent stress response alters the cytotoxic activity of hsp90-binding agents. Clin Cancer Res 6: 3312-3318, 2000.
58. Guo Y, Guettouche T, Fenna M, Boellmann F, Pratt WB, Toft DO, Smith DF and Voellmy R: Evidence for a mechanism of repression of heat shock factor 1 transcriptional activity by a multichaperone complex. J Biol Chem 276: 45791-45799, 2001.
59. Musha A, Yoshida Y, Takahashi T, Ando K, Funayama T, Kobayashi Y, Negishi A, Yokoo S and Nakano T: Synergistic effect of heat shock protein 90 inhibitor, 17-allylamino-17-demethoxygeldanamycin and X-rays, but not carbon-ion beams, on lethality in human oral squamous cell carcinoma cells. J Radiat Res (Tokyo) 53: 545-550, 2012.
60. Chang WC, Tsai PT, Lin CK, Shieh YS and Chen YW: Expression pattern of heat shock protein 90 in patients with oral squamous cell carcinoma in northern Taiwan. Br J Oral Maxillofac Surg 55: 281-286, 2017.
61. Ono K, Eguchi T, Sogawa C, Calderwood SK, Futagawa J, Kasai T, Seno M, Okamoto K, Sasaki A and Kozaki KI: HSP-enriched properties of extracellular vesicles involve survival of metastatic oral cancer cells. J Cell Biochem 119: 7350-7362, 2018.